

DOI:10.1002/ejic.201402832

# Hybrid Material Constructed from Hg(NCS)<sub>2</sub> and 2,4,6-Tris(2-pyrimidyl)-1,3,5-triazine (TPymT): Coordination of TPymT in a 2,2'-Bipyridine-Like Mode

Damir A. Safin,<sup>[a]</sup> Rebecca J. Holmberg,<sup>[a]</sup> Kevin M. N. Burgess,<sup>[a]</sup>  
Koen Robeyns,<sup>[b]</sup> David L. Bryce,<sup>[a]</sup> and Muralee Murugesu<sup>\*[a]</sup>

**Keywords:** Organic–inorganic hybrid materials / Mercury / N ligands / Coordination modes / Structure elucidation

A unique Hg<sup>II</sup> coordination polymer has been synthesized through the reaction of 2,4,6-tris(2-pyrimidyl)-1,3,5-triazine (TPymT) with a stoichiometric mixture of HgCl<sub>2</sub> and NH<sub>4</sub>NCS, thus leading to the formation of a 1D polymeric

heteroleptic hybrid material  $[\{\text{Hg}(\text{NCS})_2\}_2\text{TPymT}]_n$  (**1**). Two coordination pockets of TPymT in **1** are each coordinated to two Hg<sup>II</sup> cations in an unprecedented 2,2'-bipyridine-like mode.

## Introduction

Coordination polymers (CPs) have been known and extensively employed since the groundwork of their study was laid by Nobel Prize winner Alfred Werner.<sup>[1]</sup> He was the first to utilize such important terms as coordination numbers and coordination isomerism. Since that time, CPs were found to be an intriguing class of hybrid materials, comprising inorganic nodes and organic ligands by coordination interactions.<sup>[2]</sup> They have exhibited valuable properties and are currently employed in wide range of fields.<sup>[3]</sup> In terms of crystal engineering of CPs;  $\pi$  electron containing ligands are of ever-growing interest.

Using metal CP approaches for the preparation of organic–inorganic hybrid materials provides a synthetic interface between the properties of mononuclear complexes and bulk materials.<sup>[4]</sup> Thus, through using this technique, a wide variety of structures with unique coordination properties can be synthesized and studied. This ever-growing part of modern chemistry has shown applicability in prominent fields such as catalysis, magnetism, nonlinear optics, and molecular sensing, while still remaining a challenging field of study.<sup>[4,5]</sup> These materials are of great interest not only for their practical applications<sup>[6]</sup> but also as building units for extended structures.<sup>[7]</sup> While the organic components of coordination polymers are responsible for supramolecular and secondary interactions (e.g., hydrogen bonds,  $\pi\cdots\pi$

stacking interactions, etc.), that might be tuned in terms of molecular selectivity and recognition, the metal part mainly determines the overall geometry of the structure (e.g., dimensionality). Thus, the nature of a selected metal centre is a powerful tool to design the targeted structure. Accordingly, using the Hg<sup>II</sup> atom for the formation of hybrid materials is attractive since it is a much softer metal centre compared to its analogues (Zn<sup>II</sup> and Cd<sup>II</sup>) and, thus, promotes the formation of less predictable final structures.<sup>[8]</sup> Despite the numerous alluring applications of Hg<sup>II</sup> compounds in energy-saving light bulbs, thermometers, batteries, paper, paint, as well as in medicine, the study and formation of polymers using Hg<sup>II</sup> is comparatively limited.<sup>[4,9]</sup>

Moreover, the coordination chemistry of 2,4,6-tris(2-pyrimidyl)-1,3,5-triazine (TPymT) has been extremely poorly explored since it was first obtained about 55 years ago.<sup>[10]</sup> This might be explained by its general unavailability, poor solubility in common organic solvents, and by hydrolysis of the triazine fragment of TPymT in the presence of metal cations under mild conditions,<sup>[11]</sup> thus breaking down the ligand. However, there have been a few reports on the synthesis of TPymT complexes with Ru<sup>II</sup>,<sup>[12]</sup> Pb<sup>II</sup>,<sup>[13]</sup> Tl<sup>I</sup>,<sup>[13a]</sup> and UO<sub>2</sub><sup>II</sup>.<sup>[13a]</sup> Among them, only two crystal structures were described: a 1D polymeric chain  $[\{\text{Pb}_2(\text{TPymT})\cdot(\text{H}_2\text{O})(\text{NO}_3)_4\cdot\text{H}_2\text{O}\}]_n$  comprising dilead heteroleptic building blocks,<sup>[13a]</sup> and a discrete hexalead supramolecular aggregate  $[\text{Pb}_6(\text{TPymT})_2(\text{Lig})_3(\text{OTf})_{12}]$  {Lig = 4,6-bis[4-(propylthio)-2,2'-bipyridin-6-yl]pyrimidine}.<sup>[13a]</sup>

Thus, the coordination chemistry of TPymT remains challenging. With this in mind, we have recently turned our attention to the synthesis and study of TPymT-based coordination compounds. Very recently, we published the first crystal structure of a TPymT complex with a d-metal cation, namely, a dinuclear Cd<sup>II</sup> complex  $[\text{Cd}_2(\text{TPymT})$

[a] Department of Chemistry, University of Ottawa,  
10 Marie Curie Private, K1N 6N5, Ottawa, ON, Canada  
E-mail: m.murugesu@uottawa.ca  
<http://mysite.science.uottawa.ca/mmuruges/>

[b] Institute of Condensed Matter and Nanosciences, MOST -  
Inorganic Chemistry, Université Catholique de Louvain,  
Place L. Pasteur 1, 1348 Louvain-la-Neuve, Belgium

Supporting information for this article is available on the  
WWW under <http://dx.doi.org/10.1002/ejic.201402832>.

(H<sub>2</sub>O)<sub>6</sub>(SO<sub>4</sub>)<sub>2</sub>·H<sub>2</sub>O (2).<sup>[14]</sup> Furthermore, we also reported a pseudo-polymorph [{Pb<sub>2</sub>(TPymT)(NO<sub>3</sub>)<sub>4</sub>]<sub>n</sub> (3)<sup>[15]</sup> of a previously published lead structure.<sup>[13a]</sup>

Herein, we report on the crystal structure of a polymeric heteroleptic hybrid material [{Hg(NCS)<sub>2</sub>TPymT}]<sub>n</sub> (**1**), which was also characterized by means of FTIR, Raman, diffuse reflectance, fluorescence, solution-state <sup>1</sup>H and <sup>13</sup>C as well as <sup>199</sup>Hg solid-state NMR spectroscopy, TG/DTA, and X-ray powder diffraction analyses. Furthermore, to extensively probe the unique structural characteristics of this Hg<sup>II</sup> complex, we have drawn particular attention to the NCS<sup>-</sup> counterion, since it might show coordination versatility due to a rich variety of coordination modes (see Chart S1 in the Supporting Information).<sup>[16]</sup>

## Results and Discussion

Reaction of TPymT with a stoichiometric mixture of HgCl<sub>2</sub> and NH<sub>4</sub>NCS in water yielded blocklike crystals of the complex in 86.2% yield (Scheme 1). Crystals of **1** are poorly soluble in DMF and DMSO. Note, that all experiments listed below, except for the <sup>199</sup>Hg solid-state NMR spectroscopy, were performed on the crystalline sample of **1**.

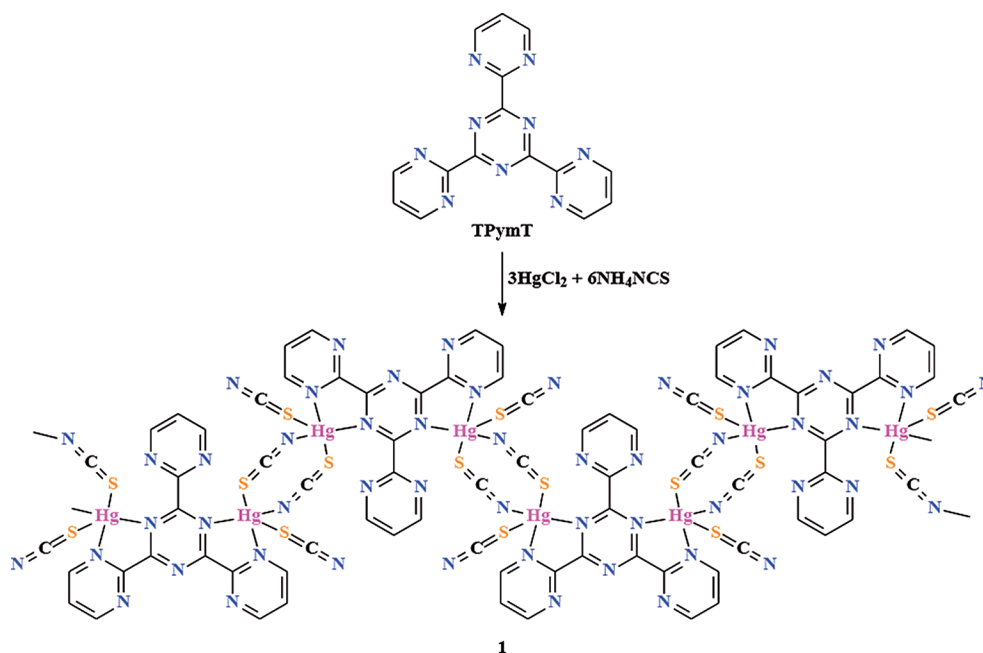
The FTIR and Raman spectra of **1** each contain bands for the aromatic C–H and C=N stretches at 3020–3040 and 1540–1560 cm<sup>-1</sup>, respectively (Figure S1 in the Supporting Information). The latter band is overlapped with a band for the aromatic ring chain vibrations, which were also found as bands at 1430–1440 and 1000 cm<sup>-1</sup>. An intense band at 2125 cm<sup>-1</sup> in the FTIR and Raman spectra of **1** was attributed to the CN stretch of the NCS<sup>-</sup> anions. This band is in the region characteristic of the S-bonded and bridging

thiocyanate ions.<sup>[16]</sup> Unfortunately, bands for the CS vibrations are obscured by the presence of the bands characteristic of the TPymT ligand<sup>[14]</sup> and, thus, cannot be identified unequivocally. The Raman spectrum of **1** also exhibits a band at 265 cm<sup>-1</sup>, corresponding to HgS vibrations.<sup>[17]</sup>

The <sup>1</sup>H NMR spectrum of **1** in [D<sub>6</sub>]DMSO contains two multiplets at 7.78–7.86 and 9.11–9.21 ppm, corresponding to the *p*- and *m*-protons, respectively, of the pyrimidine fragments. The <sup>13</sup>C NMR spectrum of **1** in the same solvent exhibits a double set of signals at about 130.0, 158.5, and 170.0 ppm, corresponding to the pyrimidine functionalities. There are also two peaks at δ = 177.6 and 178.3 ppm, arising from the triazine carbons. Furthermore, two singlets at δ = 140.4 and 142.1 ppm are indicative of the NCS<sup>-</sup> anions. Thus, the double set of signals in the <sup>13</sup>C NMR spectrum together with multiplet peaks in the <sup>1</sup>H NMR spectrum of **1** might testify to the existence of coordinated and non-coordinated pyrimidine fragments in a solution of [D<sub>6</sub>]DMSO. Two signals for the thiocyanate anions might be due to two different coordination modes.

To shed light on the electronic properties of **1**, the diffuse reflectance spectrum was recorded on a pure sample. The spectrum exhibits a broad absorption band with several maxima, accompanied by a shoulder, in the 200–600 nm range, corresponding to intraligand transitions of TPymT<sup>[14]</sup> and ligand-to-metal or metal-to-ligand charge transfer (Figure S2 in the Supporting Information).

Solid-state fluorimetric studies of **1** were undertaken to examine its photophysical properties. It was found that **1** shows a very similar emission band to that of the parent ligand TPymT<sup>[14]</sup> with maxima at around 460 and 495 nm at λ<sub>exc</sub> = 350 nm (Figure S3 in the Supporting Information). The excitation spectrum of **1**, recorded at λ<sub>em</sub> = 480 nm,



Scheme 1. Preparation of **1**.

reveals a main contribution from the band centred at about 400–425 nm. This band can be assigned to the absorption of the shoulder at about 430 nm by comparison with diffuse-reflectance spectroscopy data (Figure S2 in the Supporting Information). Thus, the observed emission of **1** is attributed to  $\pi$ - $\pi^*$  intraligand fluorescence.

The thermal properties of **1** in an air atmosphere were studied by simultaneous TG/DTA analyses to determine its stability (Figure S4 in the Supporting Information). The molecule of **1** is stable up to 250 °C and completely decomposed in three clearly defined steps. The mass loss after the first decomposition step of 5.49% is in agreement with the calculated value of 5.48%, corresponding to the elimination of cyanogen. The observed final residue of 24.57% after the second decomposition step is in excellent agreement with the value of 24.52% calculated for HgS, which is burned in an air atmosphere with the formation of elementary Hg and its further complete evaporation. The latter observation is confirmed by a broad exothermic effect, centred at 580 °C, which corresponds to a melting point (with decomposition) of HgS.<sup>[18]</sup> The thermal decomposition of **1** also reveals two low-temperature exothermic effects centred at 270 and 420 °C, corresponding to the first and second decomposition steps, respectively.

Crystals of **1** suitable for a single-crystal X-ray analysis were obtained after the synthesis on standing (1 day) with slow evaporation of the solvent. It should be noted that

several different crystals of **1** were checked by single-crystal X-ray diffraction, testifying to their identity.

According to the X-ray data, **1** crystallizes in the monoclinic space group  $C2/c$  and comprises an infinite polymeric molecule (Figure 1). It was found that TPymT in the structure of **1** is coordinated to two Hg<sup>II</sup> cations and acts as a bis(2,2'-bipyridine)-type ligand, exhibiting a bridging  $\mu_4$ -coordination mode. Complex **1** is the first example that directly shows a 2,2'-bipyridine-like coordination mode for TPymT. To date the crystal structure database contains 31 hits for the metal-containing complexes of the closest analogue of TPymT, named 2,4,6-tris(pyridin-2-yl)-1,3,5-triazine (TPT), in which the organic ligand exhibits a 2,2'-bipyridine-like coordination mode.<sup>[19]</sup> Among them, only six structures contain the TPT ligand in a bridging  $\mu_4$ -coordination mode, whereby two coordination pockets are each bonded in a 2,2'-bipyridine-like manner to a metal centre. The structural motifs  $[\text{Hg}_2\text{TPymT}]^{4+}$  are linked through bridging  $\mu_2$ -1,3-*N,S*-coordinated NCS<sup>-</sup> anions with the formation of dinuclear eight-membered metallocycles (Figure 1). These cycles are each in a chair conformation, whereby two Hg<sup>II</sup> cations deviate by about 1.42 Å from the least square plane formed by two NCS<sup>-</sup> anions (Figure S5 in the Supporting Information). As a result, 1D zig-zag-like polymeric chains are formed. These 1D chains are further stacked on top of each other (Figure 1). The Hg<sup>II</sup>...Hg<sup>II</sup> separation between two metal cations, coordinated to the

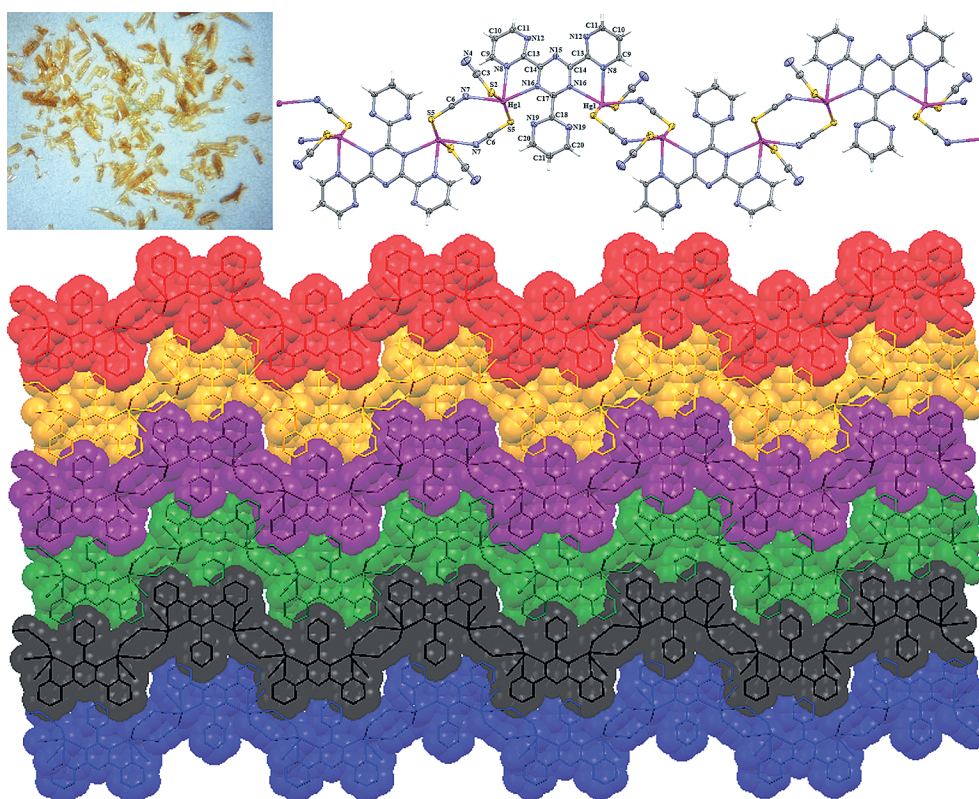


Figure 1. Photograph of crystals (top left) and molecular X-ray structure of **1** (top right) with ellipsoids drawn at the 50% probability level. Crystal packing of 1-D chains of **1** along the *a* axis (Hydrogen atoms were omitted for clarity) (bottom).

same TPymT ligand, is about 6.93 Å, while the same distance between two metal centres within the  $[\text{Hg}_2(\text{NCS})_2]^{2+}$  fragment is 5.94 Å. The shortest  $\text{Hg}^{\text{II}}\cdots\text{Hg}^{\text{II}}$  separations between neighbouring 1D chains are about 6.56 and 6.82 Å. The coordination of each  $\text{Hg}^{\text{II}}$  cation is completed by the sulfur atom of the third  $\text{NCS}^-$  anion leading to a pentacoordinate environment (Figure 1). The latter coordination sphere can be described either as square-pyramidal or trigonal-bipyramidal depending on the parameter  $\tau = (\beta - \alpha)/60$ , where  $\alpha$  and  $\beta$  are the two largest bond angles around the metal ion. An ideal square-pyramidal arrangement is described by the value of  $\tau = 0$ , while an ideal trigonal-bipyramidal arrangement has the value of  $\tau = 1$ .<sup>[20]</sup> The largest bond angles in the coordination sphere are 157.52(6) and 146.13(14)°, which give a  $\tau$  value of 0.19. This value is closer to that of a distorted square pyramid around the metal atom. The mean basal plane is occupied by two sulfur atoms, corresponding to both bridging and monodentate  $\text{NCS}^-$  anions, and two nitrogen atoms from the second  $\text{NCS}^-$  and triazine fragments. Although both Hg–S distances are very similar (ca. 2.41 Å), the Hg–N<sub>base plane</sub> bond lengths differ significantly (ca. 2.57 and 2.76 Å) (Table S1 in the Supporting Information). The apical nitrogen atom arises from the pyrimidine functionality with an Hg–N bond length of about 2.51 Å. An intriguing contact can be drawn between the Hg(1) and N(19) atoms. The non-coordinated pyrimidine fragment is situated between two  $\text{Hg}^{\text{II}}$  cations bound to the same TPymT ligand and is positioned on a twofold axis. As such, both N(19) atoms are about 2.86 Å displaced from metal centres. The interaction is out-of-plane of the pyrimidine ring and such contacts are readily observed in the CSD database.<sup>[19]</sup> It appears that this pyrimidine fragment could rotate freely to accommodate the  $\text{Hg}^{\text{II}}$  cations in the plane of the ring without steric hindrance. The long bond length (top 1% for the  $\text{Hg}^{\text{II}}\cdots\text{N}_{\text{aromatic}}$  interactions found in the CSD<sup>[19]</sup>) in combination with the inclined pyrimidine indicates that the coordination number remains 5 and that no interaction (at most a very weak interaction) should be expected between the metal centre and the N(19) atom. The dihedral angles between the planes formed by the triazine and both the coordinated and non-coordinated pyrimidine rings are about 15 and 29°, respectively. The same angles between the coordinated and non-coordinated pyrimidine planes are 32°. These angles are significantly larger than those in the structure of a discrete dinuclear  $\text{Cd}^{\text{II}}$  complex **2**<sup>[14]</sup> and a polymeric 2D complex **3**,<sup>[15]</sup> and testify to a higher distortion of the TPymT ligand in the structure of **1**. The C–S bond length is about 0.03 Å longer in favour of the monodentate  $\text{NCS}^-$  anion, while the C–N bonds are almost the same (ca. 1.16 Å) regardless of the coordination mode of the  $\text{NCS}^-$  ligands (Table S1 in the Supporting Information). This might explain the presence of the unique band, corresponding to the CN stretches of the  $\text{NCS}^-$  anions, in the FTIR spectrum of **1** (see FTIR description above, Figure S1 in the Supporting Information). The bond lengths and bond angles within the TPymT ligand in the structure of **1** are almost the same as those found in the structures of **2** and

**3**.<sup>[14,15]</sup> Closer inspection of the crystal structure of **1** revealed no classical hydrogen bonds but further  $\text{H}\cdots\text{X}$  short contacts; however, based on established criteria,<sup>[21]</sup> these weak interactions are not directing the crystal packing or molecular structures.

A bulk sample of crystalline **1** was studied by X-ray powder diffraction analysis, and the experimental X-ray powder pattern is in excellent agreement with that calculated from single-crystal X-ray diffraction (Figure S6 in the Supporting Information).

<sup>199</sup>Hg solid-state NMR experiments were performed on a bulk powder sample of **1** under cross-polarization magic-angle-spinning conditions (CP/MAS) conditions. It should be noted that the bulk powder sample was obtained using 10 times more starting material relative to the synthesis of the crystalline sample of **1**. The spectra recorded at  $B_0 = 4.7$  T reveal a large amount of chemical shift anisotropy and two crystallographically non-equivalent Hg species in the sample with the ratio 1:0.6 having isotropic chemical shifts ( $\delta_{\text{iso}}$ ) of –1130(5) and –1305(5) ppm, respectively (Figure 2). The minor component corresponds to the presence of a  $\text{Hg}(\text{SCN})_2$  byproduct ( $\delta_{\text{iso}} = -1300$  ppm).<sup>[22]</sup> Hence, **1** clearly contains one Hg site, which is in agreement with the single-crystal X-ray structure. The <sup>199</sup>Hg chemical shift tensor of **1** is characterized by the following parameters:  $\delta_{\text{iso}}$

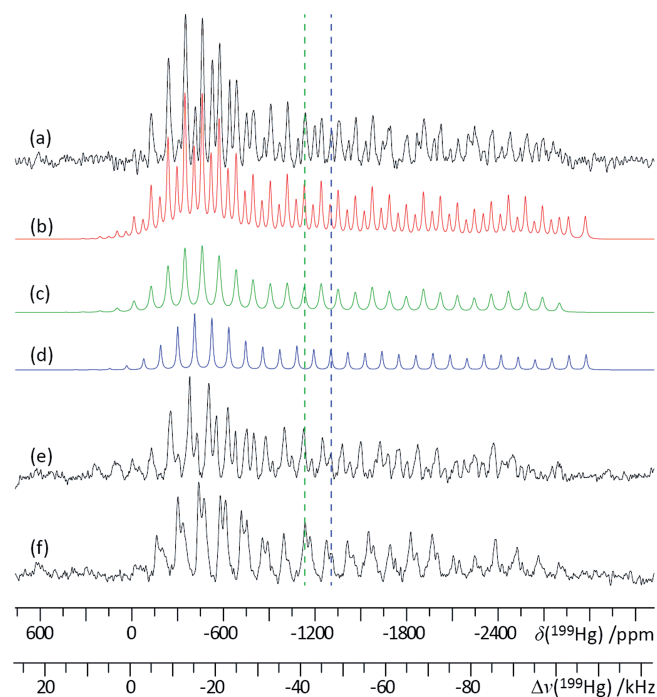


Figure 2. <sup>199</sup>Hg solid-state NMR spectra of a bulk sample of **1** acquired at  $B_0 = 4.7$  T with sample spinning rates of 4 (a), 4.5 kHz (e), and 5 kHz (f) acquired under CP/MAS conditions. The spectrum in (c) is an analytical simulation of the <sup>199</sup>Hg spectrum of **1** (see main text) and (d) is a simulation based on the previously reported NMR parameters for the  $\text{Hg}(\text{SCN})_2$  impurity ( $\delta_{\text{iso}} = -1300$  ppm).<sup>[16]</sup> The spectrum in (b) is a simulation of both **1** and  $\text{Hg}(\text{SCN})_2$  in the ratio of 1:0.6. The dashed lines indicate the position of the isotropic chemical shifts for **1** [green,  $\delta_{\text{iso}} = -1130(5)$  ppm] and  $\text{Hg}(\text{SCN})_2$  [blue,  $\delta_{\text{iso}} = -1305(5)$  ppm].

= -1130(5),  $\Omega$  = 2880(40) ppm, and  $\kappa$  = 0.75(0.05). The substantial span ( $\Omega$ ) and skew ( $\kappa$ ) values are consistent with the distorted square-pyramidal environment around Hg. The NMR parameters for **1** are nicely corroborated by density functional theory (DFT) calculations on a molecular model of **1** (Figure S7 in the Supporting Information) based on its crystal structure. Under the zeroth-order regular approximation (ZORA), as implemented in the Amsterdam Density Functional (ADF) software,<sup>[23]</sup> a calculated  $\delta_{\text{iso}}$  value of -1070 ppm is obtained when spin-orbit relativistic effects are included compared with -536 ppm when relativity is not considered in the calculations.

A powder sample of **1** was also studied by X-ray powder diffraction analysis, and the experimental X-ray powder pattern testifies to a presence of both **1** and Hg(SCN)<sub>2</sub> (Figure S6 in the Supporting Information). Surprisingly, keeping the same amount of starting compounds but using the TPymT/HgCl<sub>2</sub>/NH<sub>4</sub>NCS ratio of 1:2:4 led to the same mixture of **1** and Hg(SCN)<sub>2</sub>. However, the yield was significantly lower. The same observation was also proven by the <sup>199</sup>Hg solid-state NMR experiment.

## Conclusions

In summary, a novel 1D polymeric heteroleptic hybrid material [ $\{\text{Hg}(\text{NCS})_2\}_2\text{TPymT}\}_n$  (**1**) was synthesized and characterized by FTIR, Raman, diffuse-reflectance, fluorescence, solution-state <sup>1</sup>H and <sup>13</sup>C as well as <sup>199</sup>Hg solid-state NMR spectroscopy, TG/DTA, and X-ray powder diffraction analyses. The molecular structure of **1** was elucidated by single-crystal X-ray diffraction analysis, which revealed, to the best of our knowledge, the first structurally characterized example of a metal complex of TPymT exhibiting a 2,2'-bipyridine-like coordination mode.

## Experimental Section

**Physical Measurements:** Infrared spectra were recorded with a Varian 640 FTIR spectrometer equipped with an ATR in the 500–4000 cm<sup>-1</sup> range. Raman spectra in the solid state were obtained with a FTIR Nicolet Magna 860 with Raman unit and Nd:YVO<sub>4</sub> ( $\lambda$  = 1064 nm) laser. <sup>1</sup>H and <sup>13</sup>C NMR spectra in [D<sub>6</sub>]DMSO were obtained on a Bruker Avance 300 MHz spectrometer at 25 °C. Diffuse-reflectance spectra were obtained with a Varian Cary 100 spectrometer using polytetrafluoroethylene (PTFE) as a reference. Solid-state emission and excitation spectra were obtained with a Perkin–Elmer LS 50 luminescence spectrometer. Kubelka–Munk, emission, and excitation spectra were normalized to allow meaningful comparisons. Simultaneous thermogravimetric (TG) and differential thermal (DTA) analyses were performed by a SDT 2960 Simultaneous DTA-TGA instrument in a dynamic air atmosphere (100 mL min<sup>-1</sup>) from laboratory temperature to 900 °C with a 10 °C min<sup>-1</sup> heating rate. Elemental analyses were performed on a Perkin–Elmer 2400 CHN analyzer.

**Synthesis of 1:** A hot aqueous (12 mL) solution of a mixture of HgCl<sub>2</sub> (0.075 mmol, 0.021 g) and NH<sub>4</sub>NCS (0.15 mmol, 0.012 g) was added to a suspension of TPymT (0.025 mmol, 0.008 g) in the same solvent (20 mL). The mixture was heated at reflux until all of

the reactants dissolved. The resulting pale yellow solution was cooled to yield pale yellow blocklike crystals, yield 0.020 g (86.2%). <sup>1</sup>H NMR:  $\delta$  = 7.78–7.86 (m, 3 H, *p*-CH, pyrimidine), 9.11–9.21 (m, 6 H, *m*-CH, pyrimidine) ppm. <sup>13</sup>C NMR:  $\delta$  = 130.1 (s, *p*-C, pyrimidine), 140.4, 142.1 (s, NCS), 158.3, 158.9 (s, *m*-C, pyrimidine), 169.4, 170.1 (s, *i*-C, pyrimidine), 177.6, 178.3 (s, triazine) ppm. C<sub>19</sub>H<sub>9</sub>Hg<sub>2</sub>N<sub>13</sub>S<sub>4</sub> (948.79): calcd. C 24.05, H 0.96, N 19.19; found C 24.18, H 1.08, N 19.10.

A bulk powder sample of **1**, prepared for the <sup>199</sup>Hg solid-state NMR spectroscopy, was synthesized according to the same procedure, instead using an aqueous (100 mL) solution of a mixture of HgCl<sub>2</sub> (0.75 mmol, 0.205 g) and NH<sub>4</sub>NCS (1.50 mmol, 0.115 g), and a suspension of TPymT (0.25 mmol, 0.08 g) in the same solvent (150 mL).

**<sup>199</sup>Hg Solid-state NMR Spectroscopy:** Spectra were acquired at 4.7 T [ $\nu_{\text{L}}(^{199}\text{Hg})$  = 35.8 MHz and  $\nu_{\text{L}}(^1\text{H})$  = 200.1 MHz] using a Bruker 7 mm low-frequency double resonance (HX) probe. MAS NMR spectra were acquired at three different spinning frequencies under CP conditions with continuous-wave proton decoupling. A 3  $\mu\text{s}$  <sup>1</sup>H  $\pi/2$  pulse, a 7 ms contact time, and a 3 s recycle delay were used for all experiments. A total of 88720, 55176, and 55679 transients were acquired for the 4 kHz, 4.5 kHz, and 5 kHz spectra respectively. The <sup>199</sup>Hg chemical shift was referenced to Hg(CH<sub>3</sub>)<sub>2</sub> at 0 ppm using the secondary reference sample NEt<sub>4</sub>Na[Hg(CN)<sub>4</sub>] ( $\delta_{\text{iso}}$  = -434 ppm).<sup>[24]</sup> All spectra were baseline-corrected. It was possible to measure accurately the isotropic chemical shifts of the two Hg species present by overlaying the three experimental spectra [ $\delta_{\text{iso}}$  = -1130(5) ppm and -1305(5) ppm for the major and minor <sup>199</sup>Hg sites respectively]. Analytical simulations were generated in the WSolid1 program.

**Amsterdam Density Functional (ADF) Calculations:** DFT calculations were performed under the zeroth-order regular approximation (ZORA) as implemented in the ADF software package<sup>[23]</sup> available through the High Performance Computing Virtual Laboratory (HPCVL). The molecular model for **1** used in the calculations is depicted in Figure S6. The exchange correlation functional BP86 was used under the generalized gradient approximation (GGA). The QZ4P basis set was used on all atoms. Calculations were performed with and without spin-orbit relativistic effects. These calculations yield the isotropic magnetic shielding constant ( $\sigma_{\text{iso}}$ ). Isotropic chemical shift values were obtained by comparing to calculations performed on a shift reference (i.e.,  $\delta_{\text{iso}} = \sigma_{\text{iso,ref}} - \sigma_{\text{iso}} / (1 - \sigma_{\text{iso,ref}})$ ). For HgMe<sub>2</sub>,  $\sigma_{\text{iso,ref}}$  = 8279 and 6224 ppm when spin-orbit relativistic effects are and are not included in the calculations, respectively. The bond lengths for HgMe<sub>2</sub> are known based on previous electron diffraction studies.<sup>[25]</sup>

**X-ray Powder Diffraction Analysis:** X-ray powder diffraction analysis of the bulk sample of **1** was carried out using a Rigaku Ultima IV X-ray powder diffractometer. The parallel beam mode was used to collect the data ( $\lambda$  = 1.541836 Å).

**Single-Crystal X-ray Diffraction Analysis:** The X-ray diffraction data for **1** were collected at 150(2) K on a Mar345 image plate detector using Mo-*K*<sub>α</sub> radiation (Xenocs Fox3D mirror). The data were integrated with the crysAlisPro software.<sup>[26]</sup> The implemented empirical absorption correction was applied. The structures were solved by direct methods using the SHELXS-97 program<sup>[27]</sup> and refined by full-matrix least-squares on  $|F^2|$  using SHELXL-97.<sup>[27]</sup> Non-hydrogen atoms were refined anisotropically and the hydrogen atoms were placed on calculated positions in riding mode with temperature factors fixed at 1.2 times  $U_{\text{eq}}$  of the parent atoms. Figures were generated using the program Mercury.<sup>[28]</sup> C<sub>19</sub>H<sub>9</sub>Hg<sub>2</sub>N<sub>13</sub>S<sub>4</sub>,  $M_r$  = 948.81 g mol<sup>-1</sup>, monoclinic, space group *C2/c*,  $a$  = 6.8236(2),  $b$  =

16.9056(5),  $c = 22.4059(5)$  Å,  $\beta = 95.903(2)^\circ$ ,  $V = 2570.97(12)$  Å<sup>3</sup>,  $Z = 4$ ,  $\rho = 2.451$  g cm<sup>-3</sup>,  $\mu(\text{Mo-K}\alpha) = 12.292$  mm<sup>-1</sup>, reflections: 9041 collected, 2368 unique,  $R_{\text{int}} = 0.058$ ,  $R_1(\text{all}) = 0.0350$ ,  $wR_2(\text{all}) = 0.0970$ .

CCDC-965497 (for **1**) contains the supplementary crystallographic data. These data can be obtained free of charge from The Cambridge Crystallographic Data Centre via [www.ccdc.cam.ac.uk/data\\_request/cif](http://www.ccdc.cam.ac.uk/data_request/cif).

**Supporting Information** (see footnote on the first page of this article): Chart S1, Figures S1–S7, and Table S1.

## Acknowledgments

This work was financially supported by the Natural Sciences and Engineering Research Council of Canada – Discovery Grant (NSERC-DG), the Canada Foundation for Innovation (CFI), the Ontario Research Fund (ORF), and the Early Researcher Award (ERA).

- [1] a) Alfred Werner – Biographical, Nobelprize.org., Nobel Media AB, **2013**, Web. 26 Jan 2014; [http://www.nobelprize.org/nobel\\_prizes/chemistry/laureates/1913/werner-bio.html](http://www.nobelprize.org/nobel_prizes/chemistry/laureates/1913/werner-bio.html); b) E. C. Constable, C. E. Housecroft, *Chem. Soc. Rev.* **2013**, *42*, 1429; c) H. Werner, *Angew. Chem. Int. Ed.* **2013**, *52*, 6146; d) A.-M. Stadler, J. Harrowfield, J. Ramirez, *Polyhedron* **2013**, *52*, 1465.
- [2] See, for example: a) J. P. Zhang, X. C. Huang, X. M. Chen, *Chem. Soc. Rev.* **2009**, *38*, 2385; b) O. K. Farha, J. T. Hupp, *Acc. Chem. Res.* **2010**, *43*, 1166; c) S.-L. Zheng, X.-M. Chen, *Aust. J. Chem.* **2004**, *57*, 703.
- [3] For example: a) S. Kitagawa, R. Matsuda, *Coord. Chem. Rev.* **2007**, *251*, 2490; b) S. M. Cohen, Z. Q. Wang, *Chem. Soc. Rev.* **2009**, *38*, 1315; c) Z. B. Ma, B. Moulton, *Coord. Chem. Rev.* **2011**, *255*, 1623; d) E. Coronado, G. Mínguez Espallargas, *Chem. Soc. Rev.* **2013**, *42*, 1525; e) L. Fabbri, A. Poggi, *Chem. Soc. Rev.* **2013**, *42*, 1681; f) P. D. Frischmann, K. Mahata, F. Würthner, *Chem. Soc. Rev.* **2013**, *42*, 1847.
- [4] A. Morsali, M. Y. Masoomi, *Coord. Chem. Rev.* **2009**, *253*, 1882.
- [5] a) P. J. Hagrman, D. Hagrman, J. Zubieta, *Angew. Chem. Int. Ed.* **1999**, *38*, 2638; *Angew. Chem.* **1999**, *111*, 2798; b) J. M. Ellsworth, *Coordination Polymers: Hybrid Materials Composed of Organic Ligands and Transition Row Metals*, University of South Carolina, **2008**, p. 293.
- [6] a) C. Janiak, *Dalton Trans.* **2003**, 2781; b) S. Kitagawa, R. Kitaura, S. Noro, *Angew. Chem. Int. Ed.* **2004**, *43*, 2334; *Angew. Chem.* **2004**, *116*, 2388; c) D. Maspoch, D. Ruiz-Molina, J. Veciana, *Chem. Soc. Rev.* **2007**, *36*, 770.
- [7] B. Moulton, M. J. Zaworotko, *Chem. Rev.* **2001**, *101*, 1629.
- [8] C. Hu, I. Kalf, U. Englert, *CrystEngComm* **2007**, *9*, 603.
- [9] a) W. Levason, C. A. McAuli, *The Chemistry of Mercury*, McMillan, London, **1977**; b) Z. H. Chohan, S. K. A. Sheazi, *Synth. React. Inorg. Met.-Org. Nano-Met. Chem.* **1999**, *29*, 105; c) H. Sahebalzamani, S. Ghammamy, K. Mehrani, F. Salimi, *Der Chemica Sinica* **2010**, *1*, 39.
- [10] F. H. Case, E. Koft, *J. Am. Chem. Soc.* **1959**, *81*, 905.
- [11] a) E. I. Lerner, S. J. Lippard, *J. Am. Chem. Soc.* **1976**, *98*, 5397; b) E. I. Lerner, S. J. Lippard, *Inorg. Chem.* **1977**, *16*, 1546; c) D. Cangussu de Castro Gomes, H. O. Stumpf, F. Lloret, M. Julve, V. González, H. Adams, J. A. Thomas, *Inorg. Chim. Acta* **2005**, *358*, 1113; d) T. Glaser, H. Theil, I. Liratzis, T. Weyhermüller, E. Bill, *Inorg. Chem.* **2006**, *45*, 4889.
- [12] a) C. Metcalfe, S. Spey, H. Adams, J. A. Thomas, *J. Chem. Soc., Dalton Trans.* **2002**, 4732; b) C. Metcalfe, C. Rajput, J. A. Thomas, *J. Inorg. Biochem.* **2006**, *100*, 1314; c) E. Jakubikova, R. L. Martin, E. R. Batista, *Inorg. Chem.* **2010**, *49*, 2975.
- [13] a) E. I. Lerner, S. J. Lippard, *Inorg. Chem.* **1977**, *16*, 1537; b) A. M. Garcia, D. M. Bassani, J.-M. Lehn, G. Baum, D. Fenske, *Chem. Eur. J.* **1999**, *5*, 1234.
- [14] D. A. Safin, Y. Xu, I. Korobkov, D. L. Bryce, M. Murugesu, *CrystEngComm* **2013**, *15*, 10419.
- [15] D. A. Safin, K. M. N. Burgess, I. Korobkov, D. L. Bryce, M. Murugesu, *CrystEngComm* **2014**, *16*, 3466.
- [16] K. Nakamoto, *Infrared and Raman Spectra of Inorganic and Coordination Compounds*, part B, 5th edition, Wiley, N. Y., **1997**, p. 116.
- [17] S. Šašić, A. Antić-Jovanović, M. Jeremić, *J. Chem. Soc. Faraday Trans.* **1998**, *94*, 3255.
- [18] N. N. Greenwood, A. Earnshaw, *Chemistry of the elements*, Pergamon Press, **1984**, p. 1542.
- [19] CSD version 5.34 updates (May **2013**).
- [20] A. W. Addison, R. T. Nageswara, J. Reedijk, J. Van Rijn, G. J. Verschoor, *J. Chem. Soc., Dalton Trans.* **1984**, 1349.
- [21] T. Steiner, *Angew. Chem. Int. Ed.* **2002**, *41*, 48; *Angew. Chem.* **2002**, *114*, 50.
- [22] G. A. Bowmaker, A. V. Churakov, R. K. Harris, J. A. K. Howard, D. C. Apperley, *Inorg. Chem.* **1998**, *37*, 1734.
- [23] *Amsterdam Density Functional Software ADF2009.01 SCM*, Theoretical Chemistry, Vrije Universiteit, Amsterdam, The Netherlands, <http://www.scm.com/> **2010**.
- [24] K. Eichele, S. Kroeker, G. Wu, R. E. Wasylshen, *Solid State Nucl. Magn. Reson.* **1995**, *4*, 295.
- [25] K. Kashiwabara, S. Konaka, T. Iijima, M. Kimura, *Bull. Chem. Soc. Jpn.* **1973**, *46*, 407.
- [26] Agilent Technologies, CrysAlisPro Software System, version 1.171.34.40, Agilent Technologies UK Ltd., Oxford, UK, **2013**.
- [27] G. M. Sheldrick, *Acta Crystallogr., Sect. A* **2008**, *64*, 112.
- [28] I. J. Bruno, J. C. Cole, P. R. Edgington, M. Kessler, C. F. Macrae, P. McCabe, J. Pearson, R. Taylor, *Acta Crystallogr., Sect. B* **2002**, *58*, 389.

Received: September 2, 2014

Published Online: ■

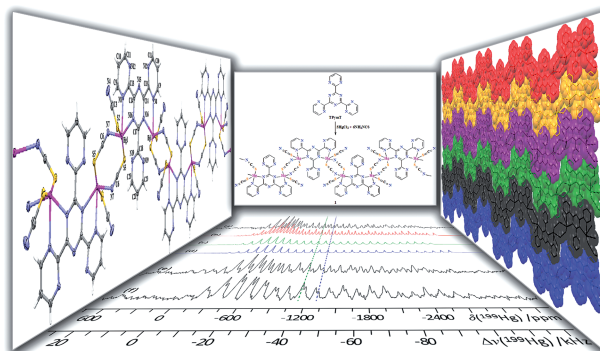
## Hybrid Material

D. A. Safin, R. J. Holmberg,  
K. M. N. Burgess, K. Robeyns,  
D. L. Bryce, M. Murugesu\* ..... 1–7



Hybrid Material Constructed from  $\text{Hg}(\text{NCS})_2$  and 2,4,6-Tris(2-pyrimidyl)-1,3,5-triazine (TPymT): Coordination of TPymT in a 2,2'-Bipyridine-Like Mode

**Keywords:** Organic–inorganic hybrid materials / Mercury / N ligands / Coordination modes / Structure elucidation



Reaction of 2,4,6-tris(2-pyrimidyl)-1,3,5-triazine (TPymT) with a mixture of  $\text{HgCl}_2$  and  $\text{NH}_4\text{NCS}$  leads to the formation of a polymeric heteroleptic hybrid material

$[\{\text{Hg}(\text{NCS})_2\}_2\text{TPymT}]_n$ , in which two coordination pockets of TPymT are each coordinated to two  $\text{Hg}^{\text{II}}$  cations in an unprecedented 2,2'-bipyridine-like mode.